Physics Letters B 742 (2015) 285–289

Contents lists available at ScienceDirect

Physics Letters B

www.elsevier.com/locate/physletb

Deuteron–deuteron scattering above four-nucleon breakup threshold

A. Deltuva [a,*], A.C. Fonseca [b]

[a] Institute of Theoretical Physics and Astronomy, Vilnius University, A. Goštauto 12, LT-01108 Vilnius, Lithuania
[b] Centro de Física Nuclear da Universidade de Lisboa, P-1649-003 Lisboa, Portugal

ARTICLE INFO

Article history:
Received 26 September 2014
Received in revised form 11 January 2015
Accepted 29 January 2015
Available online 3 February 2015
Editor: J.-P. Blaizot

Keywords:
Four-nucleon
Scattering
Transfer reactions
Polarization

ABSTRACT

Deuteron–deuteron elastic scattering and transfer reactions in the energy regime above four-nucleon breakup threshold are described by solving exact four-particle equations for transition operators. Several realistic nuclear interaction models are used, including the one with effective many-nucleon forces generated by the explicit Δ-isobar excitation; the Coulomb force between protons is taken into account as well. Differential cross sections, deuteron analyzing powers, outgoing nucleon polarization, and deuteron-to-neutron polarization transfer coefficients are calculated at 10 MeV deuteron energy. Overall good agreement with the experimental data is found. The importance of breakup channels is demonstrated.

1. Introduction

The pursuit for numerical solutions of the three- and four-nucleon scattering problems has been, since the early seventies of the last century, one of the most challenging endeavors in nuclear reaction theory, following the development of formal exact N-body equations using momentum or configuration space representations [1,2]. Progress advanced slowly at first and limited to the use of separable representations of subsystem operators, but with the advent of powerful computational tools, both in terms of algorithms (spline interpolation, Padé summation, special integration meshes and weights, etc.) and hardware advances, three-nucleon (3N) calculations with realistic nucleon–nucleon (NN) force models reached state-of-the-art status in the early 1990s due to the effort of a number of independent groups [3–7]. Due to its higher dimensionality and multichannel complexity, the four-nucleon (4N) scattering problem took twenty years longer to reach the same status as the three-nucleon system except for the calculation of breakup amplitudes. These developments are mainly due to the works of the Pisa [8–11], Grenoble–Strasbourg [12–15], and Lisbon [16–19] groups. Because the first two groups use the coordinate-space representation, they were able to include, not only realistic two-body interactions, but also realistic three-body force models. Nevertheless they have had a major difficulty in calculating multichannel reactions and going beyond breakup threshold, particularly when the Coulomb interaction is included between protons. The Lisbon group uses the momentum space Alt, Grassberger and Sandhas (AGS) equations for transition operators [2] that can be solved for multichannel reactions both below and above breakup and with the Coulomb force included. The only stumbling block has been the inclusion of irreducible three-body forces. As alternative the nuclear force model with explicit excitation of a nucleon to a Δ isobar was used. This coupling generates both effective three- and four-nucleon forces (3NF and 4NF) that have been successfully included in 4N calculations by the Lisbon–Hannover Collaboration [20]. The calculations using potentials derived from chiral effective field theory have been performed as well [16,17] but so far including only the NN part of the interaction.

In the last 40 years progress in nuclear reaction theory has most often succeeded experimental developments to the point that, when calculations achieved a solid ground, the instrumentation that gave rise to the data was no longer in operation. Therefore inconsistencies between different data cannot anymore be resolved by repeating the experiments or developing new ones guided by the theoretical predictions. The 4N scattering problem has suffered from this much more than the 3N system for the reasons mentioned above. Nevertheless, new 4N scattering calculations are worth pursuing because they lead the way to the solution on complex multiparticle scattering problems, not just in nuclear physics but also in cold atom physics [21].

In this work we present first results for 4N reactions initiated by the collision of two deuterons (d) at energies above four-particle breakup threshold. In this energy domain there are a few shallow resonances [22]; therefore one does not expect the same problems

* Corresponding author.
E-mail address: arnoldas.deltuva@tfai.vu.lt (A. Deltuva).

http://dx.doi.org/10.1016/j.physletb.2015.01.052

as encountered in n-^{3}H and n-^{3}He near threshold. However, in two aspects the theoretical description of the $d+d$ scattering is even more interesting and challenging. First, since deuterons are loosely bound and spatially large systems, the scattering of two deuterons looks like the collision of two identical halo nuclei. The coupling to breakup channels in such a system is considerably stronger than in nucleon–trinucleon scattering. This makes the $d+d$ reactions computationally more difficult since open breakup channels lead to most complicated singularities in the kernel of scattering equations and, furthermore, a larger number of partial waves is needed. Second, the deuteron being a spin one particle also provides the opportunity to calculate a number of tensor observables, both in $d+d$ elastic as well as in ^{2}H$(d,p)^3$H and ^{2}H$(d,n)^3$He transfer reactions for which there is experimental data. The most abundant set of the experimental data for $d+d$ reactions exists at deuteron energy $E_d = 10$ MeV where not only differential cross section and analyzing powers but also deuteron-to-neutron polarization transfer coefficients have been measured [23] establishing the ^{2}H$(d,n)^3$He reaction as an efficient source for polarized neutrons.

In Section 2 we explain the AGS equations we use and how to solve them. In Section 3 we show results for $d+d$ elastic scattering, while in Section 4 results for ^{2}H$(d,p)^3$H and ^{2}H$(d,n)^3$He transfer reactions are presented. Conclusions are drawn in Section 5.

2. Deuteron–deuteron scattering equations

As in our previous studies of 4N scattering [16,24,19], we take advantage of the isospin symmetry and treat protons and neutrons as identical fermions. This enables the symmetrization of the transition operators $\mathcal{U}_{\beta\alpha}$ thereby reducing the number of components that are distinct according to two-cluster partitions [16]. As usual, $\alpha = 1$ labels the $3+1$ partition (12,3)4, while $\alpha = 2$ stands for the $2+2$ partition (12)(34). To ensure the required full antisymmetry of the four fermion system, the employed basis states have to be antisymmetric under the exchange of two particles in subsystem (12), and also in the subsystem (34) for the $2+2$ partition. The 4N transition operators $\mathcal{U}_{\beta 2}$ describing deuteron–deuteron scattering obey the AGS integral equations

$$\mathcal{U}_{12} = (G_0 t G_0)^{-1} - P_{34} U_1 G_0 t G_0 \mathcal{U}_{12} + U_2 G_0 t G_0 \mathcal{U}_{22}, \tag{1a}$$

$$\mathcal{U}_{22} = (1 - P_{34}) U_1 G_0 t G_0 \mathcal{U}_{12}. \tag{1b}$$

Here P_{34} is the permutation operator of particles 3 and 4,

$$t = v + v G_0 t \tag{2}$$

is two particle transition operator for the pair (12) interacting via potential v, while U_1 and U_2 are symmetrized transition operators for $3+1$ and $2+2$ subsystems, respectively [16]. The dependence of all transition operators on the available energy E arises through the free four-particle resolvent

$$G_0 = (E + i\varepsilon - H_0)^{-1}, \tag{3}$$

with H_0 being the free Hamiltonian. The finite imaginary part $i\varepsilon$ is introduced in the complex energy method to avoid singularities in the kernel of AGS equations, but the limit $\varepsilon \to +0$ is needed for physical amplitudes, that are given by the on-shell matrix elements of the transition operators $\mathcal{U}_{\beta\alpha}$ [16]. The $\varepsilon \to +0$ limit is obtained by the analytic continuation of the finite ε results using the point method [25]. The analytic continuation, however, is only accurate when using sufficiently small ε values at which the kernel of the AGS equations, although formally being nonsingular, still shows a quasisingular behavior [18]. These quasisingularities reflect the presence of open $p + {}^3$H, $n + {}^3$He, $d+d$, $d+n+p$, and $n+n+p+p$ channels. Their treatment is taken over from Ref. [18] where a special method for numerical integration absorbing the quasisingular factor into the integration weights was developed. This way the quasisingularities can be integrated accurately without increasing significantly the number of grid points. In the present calculations we obtain well converged results using ε between 1.2 and 3.0 MeV in 0.3 MeV steps and about 30 grid points for the discretization of each momentum variable. Note that due to a larger weight of breakup channels a bit more ε values (about 6) are needed for a reliable $\varepsilon \to +0$ extrapolation as compared to previous calculations [18,26].

Although we explore the isospin symmetry, we also account for the isospin violation effects due to the pp Coulomb repulsion and the hadronic charge dependence (CD) of the nuclear force. These effects cause the two-nucleon transition matrix t to couple the states with different total isospin in both 3N and 4N systems. In 3N or 4N total isospin basis, the two-nucleon transition matrix t is given by linear combinations of pp, np, and nn transition operators as described in Ref. [27]. For the pp pair beside the nuclear force also the screened Coulomb potential is added, enabling rigorous inclusion of the Coulomb interaction in the deuteron–deuteron scattering via the method of screening and renormalization [28,29,24]. We obtain fully converged results calculating the Coulomb-distorted short-range part of the amplitudes with the screening radius $R = 13$ fm. The direct unscreened Coulomb amplitude is present only in the elastic scattering; it is added after the renormalization of the short-range amplitude. The direct Coulomb amplitude causes the $d+d$ elastic differential cross section to diverge in the forward and backward direction but is absent for transfer reactions that are only distorted by Coulomb [24]. Other electromagnetic effects as the magnetic moment interaction are not explicitly included in the calculations, however, their short-range part is implicitly included in the employed NN potentials that are fitted to the NN data. They are not isolated in the present work but, based on previous studies [17,30] where they have been found to affect the vector analyzing powers only and to decrease with increasing energy, at 10 MeV one could expect only minor effects.

We solve the AGS equations in the momentum-space partial-wave framework following the methodology developed in Refs. [16,18]. In this framework the AGS equations constitute a large system of coupled integral equations in three continuous Jacobi momentum variables. The integrals are discretized using Gaussian quadratures with special (standard) weights for quasisingular (nonsingular) integrands, leading to a huge system of linear algebraic equations. Beside the number of grid points that can be kept moderate, the size of the resulting system depends also on the number of included angular momentum states. With respect to the number of partial waves needed for achieving convergence, the $d+d$ reactions are more demanding than those initiated by the $p + {}^3$H or $n + {}^3$He collisions already calculated in Refs. [19,27]. In terms of the basis states defined in Refs. [31,27], when solving the AGS equations we include 4N partial waves with orbital angular momenta l_x up to 6 and l_y, l_z up to 7, total angular momenta of the 2N subsystem j_x, j_y up to 6, total angular momentum of the 3N subsystem J_y up to $\frac{13}{2}$, and total 4N angular momentum $\mathcal{J}$ up to 7. Once the AGS equations are solved, for the calculation of elastic observables it is sufficient to include only the initial and final $d+d$ states with $l_z \le 4$. In contrast, transfer reactions ^{2}H$(d,p)^3$H and ^{2}H$(d,n)^3$He require l_z at least up to 6 in the channel states.

3. Elastic scattering

As in our previous calculations of nucleon–trinucleon scattering, we use several realistic nuclear force models, enabling us to

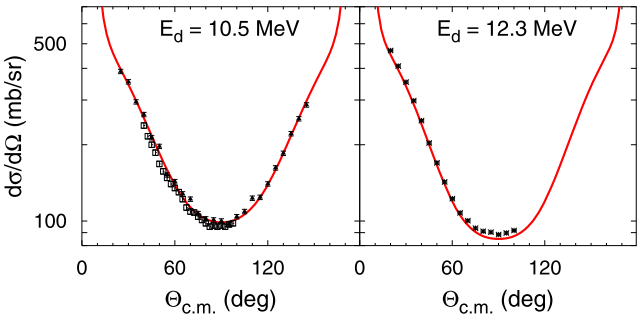

Fig. 1. Differential cross section of $d+d$ elastic scattering at 10.5 and 12.3 MeV deuteron energy. Results calculated using INOY04 potential are compared with experimental data from Refs. [35] (□), [36] (▲), and [37] (×).

study the sensitivity of the predictions to the dynamic input. Beside two purely nucleonic interaction models, the inside-nonlocal outside-Yukawa (INOY04) potential by Doleschall [32,13] and the CD Bonn potential [33], we also use the two-baryon potential CD Bonn + Δ [34] that is the coupled-channel extension of CD Bonn, explicitly allowing virtual excitation of a nucleon to a Δ isobar and thereby yielding mutually consistent effective three- and four-nucleon forces. This model, however, is not fitted to the trinucleon binding energy (BE), yielding 7.53 (8.28) MeV for ^{3}He (^{3}H) which is increased relative to the CD Bonn BE result of 7.26 (8.00) MeV. Only the INOY04 model, predicts the BE of ^{3}He (^{3}H) to be 7.73 (8.49) MeV, nearly reproducing the experimental value of 7.72 (8.48) MeV. Since the $p+{}^3$H and $n+{}^3$He threshold positions depend on the respective BE, some scattering observables are expected to correlate with the BE, thereby establishing INOY04 as a reference potential. Of course, the dependence of the observables on the used interaction model is in general much more complicated, but in particular cases simple correlations with nonmeasurable bound state properties such as the deuteron D-wave probability P_D may take place. For the INOY04 potential $P_D = 3.60\%$ while CD Bonn and CD Bonn + Δ have $P_D = 4.85\%$.

In the present work we concentrate on the $d+d$ scattering at deuteron energy $E_d = 10$ MeV where the most abundant set of experimental data exists, both for elastic and transfer reactions. The differential cross section $d\sigma/d\Omega$ for elastic $d+d$ scattering is, however, an exception. We therefore show $d\sigma/d\Omega$ as a function of the center of mass (c.m.) scattering angle $\Theta_{\rm c.m.}$ in Fig. 1 at $E_d = 10.5$ and 12.3 MeV. Solely the INOY04 potential is used for predictions but, based on the study at $E_d = 10$ MeV, the sensitivity of this observable to the force model is small. The angular dependence of $d\sigma/d\Omega$ is simple, with forward and backward peaks, where $d\sigma/d\Omega$ diverges due to the long-range Coulomb amplitude, and a minimum at $\Theta_{\rm c.m.} = 90°$. This shape remains almost constant while the absolute value of the differential cross section decreases with increasing energy. Regarding the description of the experimental data, the picture is a bit contradictory. At $E_d = 10.5$ MeV there is a good agreement with the data from Ref. [36] while the data from Ref. [35] are slightly overpredicted, by 3% at $\Theta_{\rm c.m.} = 90°$. At $E_d = 12.3$ MeV the data from Ref. [37] are well reproduced by the calculations at $\Theta_{\rm c.m.} < 65°$ but slightly underpredicted around the minimum, by 4% at $\Theta_{\rm c.m.} = 90°$. These findings suggest that more calculations over a wider energy range need to be performed and compared with the available data to determine the discrepancies between theory and experiment and find out possible inconsistencies between data sets.

In Fig. 2 we present results for deuteron vector analyzing power iT_{11} and tensor analyzing powers T_{20}, T_{21}, and T_{22} in $d+d$ elastic scattering at $E_d = 10$ MeV. The predictions are obtained using the potential models INOY04, CD Bonn + Δ, and CD Bonn. These spin observables are very small in their absolute value, of the order of 0.02. Due to the identity of the two deuterons the angular distributions of elastic observables in the c.m. frame are either symmetric ($d\sigma/d\Omega$, T_{20}, T_{22}) or antisymmetric (iT_{11}, T_{21}) with respect to $\Theta_{\rm c.m.} = 90°$. The overall description of the experimental data is good. The data have relatively large error bars, especially in the iT_{11} case where two data sets [38,39] are available. The symmetric analyzing powers T_{20} and T_{22} are most sensitive to the employed force model. However, the results obtained with different potentials do not correlate with the properties of 2N and 3N bound states such as binding energies or deuteron D-state probability. The data are reproduced best by the predictions using the CD Bonn + Δ potential. The Δ-isobar effect is especially significant and beneficial for T_{20}. The antisymmetric analyzing powers iT_{11} and T_{21} show less sensitivity to the employed potential. At least to some extent this is due to kinematic reasons, since iT_{11} are T_{21} vanish exactly at $\Theta_{\rm c.m.} = 90°$ where $d\sigma/d\Omega$ has its minimum and the model dependence of symmetric analyzing powers reaches its maximum.

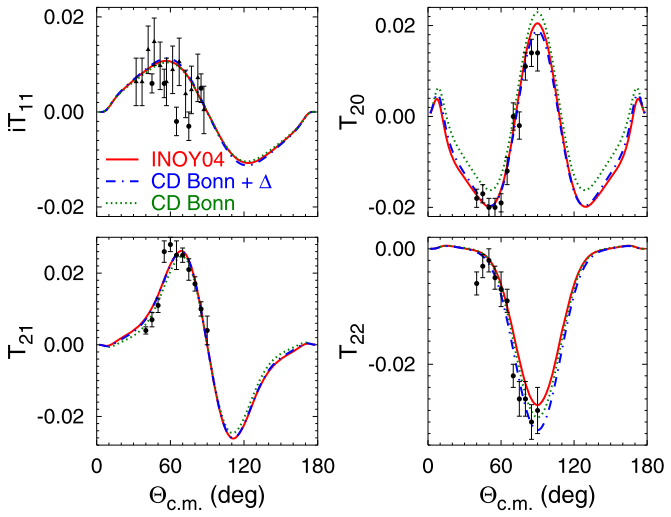

Fig. 2. Deuteron analyzing powers in $d+d$ elastic scattering at $E_d = 10$ MeV. Results obtained with potentials INOY04 (solid curves), CD Bonn + Δ (dashed–dotted curves), and CD Bonn (dotted curves) are compared with data from Refs. [38] (●) and [39] (▲).

4. Transfer reactions

We calculate the transfer reactions ^{2}H$(d,p)^3$H and ^{2}H$(d,n)^3$He using the same nuclear interaction models, i.e., INOY04, CD Bonn + Δ, and CD Bonn. In Fig. 3 we present results at $E_d = 10.0$ and 12.3 MeV for the differential cross section $d\sigma/d\Omega$ as function of the nucleon scattering angle $\Theta_{\rm c.m.}$ in the c.m. frame. For both ^{2}H$(d,p)^3$H and ^{2}H$(d,n)^3$He reactions, $d\sigma/d\Omega$ has very similar shape but is slightly higher for the latter. The differential cross section is symmetric with respect to $\Theta_{\rm c.m.} = 90°$ but has a more complicated angular and energy dependence than in the case of elastic scattering. At both considered energies there are forward and backward peaks as well as local minima around $\Theta_{\rm c.m.} = 45°$ and 135°. At $E_d = 10.0$ MeV there is just a local maximum located at $\Theta_{\rm c.m.} = 90°$ which evolves into a shallow local minimum as the energy increases to 12.3 MeV; meanwhile two local maxima appear around $\Theta_{\rm c.m.} = 70°$ and 110°. Such a behavior is seen also in the experimental data [37,40–42]. The overall agreement between theoretical results and the data is good, except at intermediate angles where $d\sigma/d\Omega$ is small and the data are slightly underpredicted by the INOY04 results, roughly by 6% at $\Theta_{\rm c.m.} = 90°$. The sensitivity to the employed potential models is studied at $E_d = 10.0$ MeV and is visible around the extrema of $d\sigma/d\Omega$. While

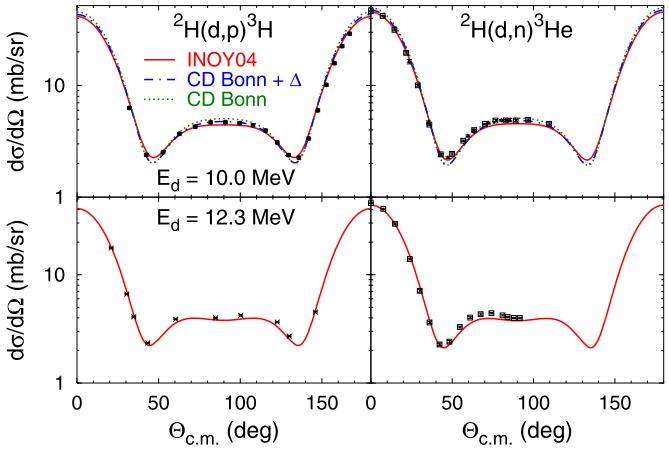

Fig. 3. Differential cross section of ^{2}H(d, p)^{3}H (left) and ^{2}H(d, n)^{3}He (right) transfer reactions at 10.0 and 12.3 MeV deuteron energy. Curves are as in Fig. 2. The data are from Refs. [40] (•), [37] (×), [41] (□), and [42] (▲).

Table 1
Predicted total cross sections for ^{2}H(d, p)^{3}H and ^{2}H(d, n)^{3}He transfer reactions and for breakup, labeled σ_p, σ_n, and σ_b, respectively, all in millibarns, at 10 MeV deuteron energy.

	σ_p	σ_n	σ_b
CD Bonn	83.4	87.1	110
CD Bonn + Δ	79.8	83.9	113
INOY04	77.6	81.3	112

at forward and backward peaks and central maximum the predictions roughly scale with the trinucleon BE as already observed in previous calculations below breakup threshold [24,43], at the minima CD Bonn and CD Bonn + Δ results are indistinguishable. This may indicate a possible sensitivity to two-nucleon isospin singlet partial waves since there CD Bonn and CD Bonn + Δ potentials are identical.

The resulting total cross sections σ_p and σ_n at $E_d = 10$ MeV are collected in Table 1 for all three potentials. The total transfer cross sections scale quite well with the trinucleon BE. In addition we present also the total breakup cross section σ_b, including both three- and four-cluster channels. It is calculated using the optical theorem with finite screening radius R before subtraction and renormalization of the elastic scattering amplitude because transfer and breakup operators are short-ranged and the respective total cross sections are unchanged by renormalization phases [44]. Already at $E_d = 10$ MeV σ_b exceeds σ_p and σ_n, indicating the importance of breakup in $d+d$ collisions. Note that in $n+^3$He scattering breakup becomes the dominant inelastic channel only above the neutron laboratory energy of 23 MeV which roughly corresponds to $E_d = 28$ MeV.

Next we consider single-polarization spin observables in ^{2}H($\boldsymbol{d}$, p)^{3}H and ^{2}H($\boldsymbol{d}$, n)^{3}He reactions at $E_d = 10$ MeV. In Fig. 4 we show vector analyzing power iT_{11}, tensor analyzing powers T_{20}, T_{21}, and T_{22}, and outgoing nucleon polarization P_y calculated using INOY04, CD Bonn + Δ, and CD Bonn potentials. All deuteron analyzing powers exhibit a complex angular dependence with several local minima and maxima. They show no symmetry with respect to $\Theta_{c.m.} = 90°$, in contrast to P_y which is antisymmetric. The differences between ^{2}H($\boldsymbol{d}$, p)^{3}H and ^{2}H($\boldsymbol{d}$, n)^{3}He observables are quite small but visible, e.g., around second maximum of T_{20}. For most observables several measurements exist [40,45–49,23] that are at variance in particular cases, especially for iT_{11}. Nevertheless, the overall description of the experimental data by our calculations is successful with only few small or at most moderate disagreements, mostly in the vector observables: the minima of iT_{11} are underpredicted while the positive peak of P_y is shifted to larger angles. The sensitivity to the used interaction model is quite small; it is most visible for iT_{11}. It is not a simple scaling with trinucleon BE since often CD Bonn and CD Bonn + Δ predictions stay quite close together with INOY04 being further away. This may again indicate the dominance of NN isospin singlet partial waves. It may even indicate partial correlation of the observables with the deuteron D-state probability P_D, but more detailed studies are needed to confirm or reject this speculation.

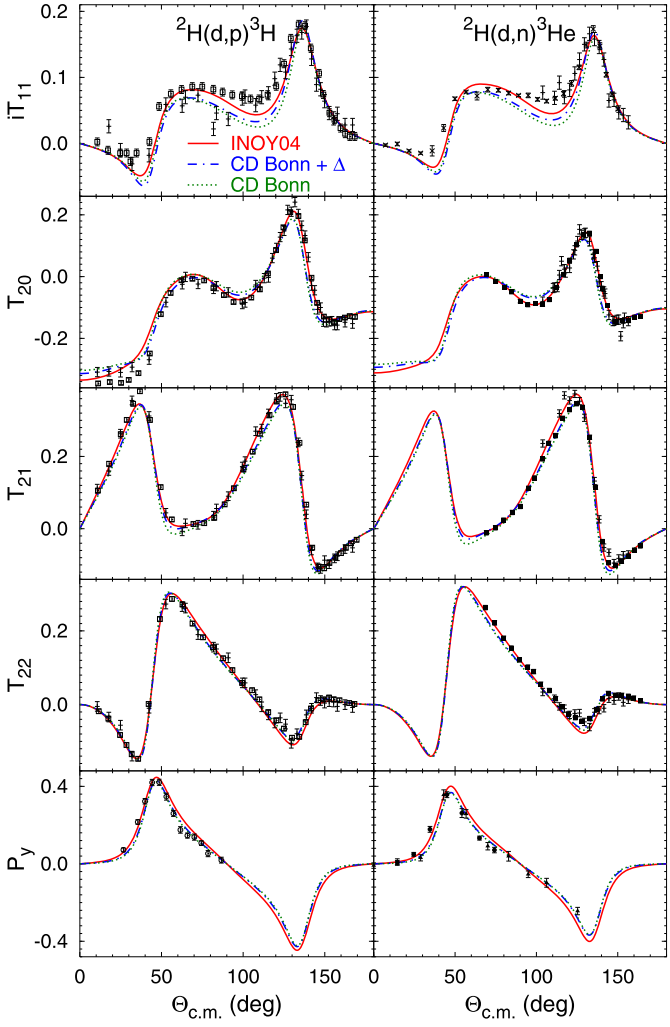

Fig. 4. Deuteron analyzing powers and outgoing nucleon polarization of ^{2}H($\boldsymbol{d}$, p)^{3}H (left) and ^{2}H($\boldsymbol{d}$, n)^{3}He (right) transfer reactions at 10 MeV deuteron energy. Curves are as in Fig. 2. The data are from Refs. [40] (+), [45] (□), [46] (×), [47] (■), [48] (○), [49] (•), and [23] (▲).

Finally we show the results for double-polarization observables. Deuteron-to-neutron polarization transfer coefficients $K_x^{x'}$, $K_x^{z'}$, $K_z^{x'}$, $K_z^{z'}$, $K_y^{y'}$, and $K_{yy}^{y'}$ in the ^{2}H($\boldsymbol{d}$, $\boldsymbol{n}$)^{3}He reaction at $E_d = 10$ MeV have been measured in Ref. [23]. These data and our predictions based on three nuclear interaction models are compared in Fig. 5. The polarization transfer coefficients exhibit a very complex angular dependence having up to six local extrema. Given such a complicated behavior of the observables the found agreement between theory and experiment is impressive. There are only small discrepancies such as a slight underestimation of $K_y^{y'}$ at intermediate angles. The model dependence of the polarization transfer coefficients is quite weak and qualitatively the same as already seen for single-polarization observables.

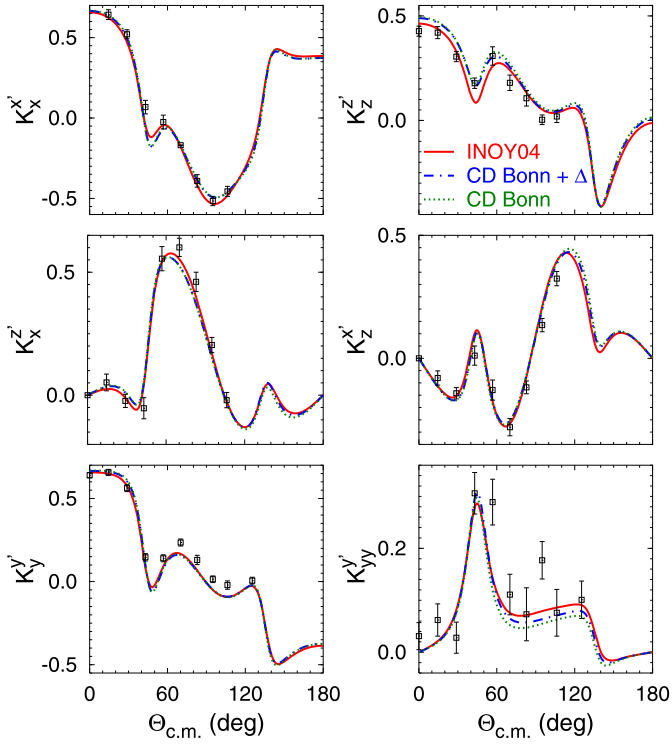

Fig. 5. Deuteron-to-neutron polarization transfer coefficients of ^{2}H($\boldsymbol{d}$, $\boldsymbol{n}$)^{3}He reaction at 10 MeV deuteron energy. Curves are as in Fig. 2. The data are from Ref. [23].

5. Conclusions

We perform calculations for elastic and transfer reactions initiated by deuteron–deuteron collisions above four-nucleon breakup threshold. This process mimics the scattering of two halo nuclei. As dynamic input we use several realistic two-nucleon potentials and include the proton–proton Coulomb force via the screening and renormalization method. Exact four-particle scattering equations in the integral form for symmetrized transition operators are solved in the momentum-space framework where the presence of open breakup channels leads to a kernel with a highly nontrivial singularity structure. The complex energy method with special integration weights is successfully applied to deal with this difficulty. Compared to previous calculations of nucleon–trinucleon scattering, the relatively weak binding of deuteron and its large spatial size lead to additional complications such as a slower partial-wave and complex-energy convergence. Nevertheless, we obtain fully converged results for $d+d$ elastic scattering as well as for ^{2}H$(d,p)^3$H and ^{2}H$(d,n)^3$He transfer reactions. For these reactions at 10 MeV deuteron energy we calculate the differential cross section and all deuteron analyzing powers; the former observable is predicted also at $E_d = 12.3$ MeV. Furthermore, for transfer reactions we calculate also the outgoing nucleon polarization and, in the ^{2}H$(d,n)^3$He case, deuteron-to-neutron polarization transfer coefficients. The overall description of the experimental data is good, even for the most complicated double-polarization observables. The comparison of predictions based on INOY04, CD Bonn + Δ, and CD Bonn potential models may indicate the dominance of NN isospin singlet partial waves for most spin observables in transfer reactions, but not in the case of elastic scattering. We also predicted the total breakup cross section and demonstrated the increased importance of breakup channels in $d+d$ reactions.

Together with the previous achievements in the nucleon–trinucleon scattering, the present work demonstrates that numerically exact calculations of all two-cluster reactions in the four-nucleon system are now possible in a fully converged way using realistic nuclear interactions and including the pp Coulomb repulsion.

References

[1] O.A. Yakubovsky, Yad. Fiz. 5 (1967) 1312;
O.A. Yakubovsky, Sov. J. Nucl. Phys. 5 (1967) 937.
[2] P. Grassberger, W. Sandhas, Nucl. Phys. B 2 (1967) 181;
E.O. Alt, P. Grassberger, W. Sandhas, JINR report No. E4-6688, 1972.
[3] Y. Koike, Y. Taniguchi, Few-Body Syst. 1 (1986) 13.
[4] C.R. Chen, G.L. Payne, J.L. Friar, B.F. Gibson, Phys. Rev. C 39 (1989) 1261.
[5] J.L. Friar, et al., Phys. Rev. C 42 (1990) 1838.
[6] T. Cornelius, W. Glöckle, J. Haidenbauer, Y. Koike, W. Plessas, H. Witała, Phys. Rev. C 41 (1990) 2538.
[7] A. Kievsky, S. Rosati, W. Tornow, M. Viviani, Nucl. Phys. A 607 (1996) 402.
[8] M. Viviani, A. Kievsky, S. Rosati, E.A. George, L.D. Knutson, Phys. Rev. Lett. 86 (2001) 3739.
[9] A. Kievsky, S. Rosati, M. Viviani, L.E. Marcucci, L. Girlanda, J. Phys. G 35 (2008) 063101.
[10] M. Viviani, R. Schiavilla, L. Girlanda, A. Kievsky, L.E. Marcucci, Phys. Rev. C 82 (2010) 044001.
[11] M. Viviani, L. Girlanda, A. Kievsky, L.E. Marcucci, Phys. Rev. Lett. 111 (2013) 172302.
[12] R. Lazauskas, PhD thesis, Université Joseph Fourier, Grenoble, 2003, http://tel.ccsd.cnrs.fr/documents/archives0/00/00/41/78/.
[13] R. Lazauskas, J. Carbonell, Phys. Rev. C 70 (2004) 044002.
[14] R. Lazauskas, Phys. Rev. C 79 (2009) 054007.
[15] R. Lazauskas, Phys. Rev. C 86 (2012) 044002.
[16] A. Deltuva, A.C. Fonseca, Phys. Rev. C 75 (2007) 014005.
[17] A. Deltuva, A.C. Fonseca, Phys. Rev. Lett. 98 (2007) 162502.
[18] A. Deltuva, A.C. Fonseca, Phys. Rev. C 86 (2012) 011001(R).
[19] A. Deltuva, A.C. Fonseca, Phys. Rev. Lett. 113 (2014) 102502.
[20] A. Deltuva, A.C. Fonseca, P.U. Sauer, Phys. Lett. B 660 (2008) 471.
[21] A. Deltuva, Phys. Rev. A 82 (2010) 040701(R).
[22] D.R. Tilley, H. Weller, G.M. Hale, Nucl. Phys. A 541 (1992) 1.
[23] G. Salzman, G.G. Ohlsen, J. Martin, J. Jarmer, T. Donoghue, Nucl. Phys. A 222 (1974) 512.
[24] A. Deltuva, A.C. Fonseca, Phys. Rev. C 76 (2007) 021001(R).
[25] L. Schlessinger, Phys. Rev. 167 (1968) 1411.
[26] A. Deltuva, A.C. Fonseca, Phys. Rev. C 87 (2013) 054002.
[27] A. Deltuva, A.C. Fonseca, Phys. Rev. C 90 (2014) 044002.
[28] J.R. Taylor, Nuovo Cimento B 23 (1974) 313;
M.D. Semon, J.R. Taylor, Nuovo Cimento A 26 (1975) 48.
[29] E.O. Alt, W. Sandhas, Phys. Rev. C 21 (1980) 1733.
[30] A. Kievsky, M. Viviani, L.E. Marcucci, Phys. Rev. C 69 (2004) 014002.
[31] A. Deltuva, Phys. Rev. A 85 (2012) 012708.
[32] P. Doleschall, Phys. Rev. C 69 (2004) 054001.
[33] R. Machleidt, Phys. Rev. C 63 (2001) 024001.
[34] A. Deltuva, R. Machleidt, P.U. Sauer, Phys. Rev. C 68 (2003) 024005.
[35] A. Wilson, M. Taylor, J. Legg, G. Phillips, Nucl. Phys. A 126 (1969) 193.
[36] L. Rosen, J.C. Allred, Phys. Rev. 88 (1952) 431.
[37] N. Jarmie, J.H. Jett, Phys. Rev. C 10 (1974) 54.
[38] W. Grüebler, V. König, R. Risler, P. Schmelzbach, R. White, P. Marmier, Nucl. Phys. A 193 (1972) 149.
[39] G. Plattner, L. Keller, Phys. Lett. B 30 (1969) 327.
[40] W. Grüebler, V. König, P.A. Schmelzbach, R. Risler, R.E. White, P. Marmier, Nucl. Phys. A 193 (1972) 129.
[41] M. Drosg, Nucl. Sci. Eng. 67 (1978) 190; in EXFOR Database (NNDC, Brookhaven, 1978).
[42] S. Thornton, Nucl. Phys. A 136 (1969) 25.
[43] A. Deltuva, A.C. Fonseca, Phys. Rev. C 81 (2010) 054002.
[44] A. Deltuva, A.C. Fonseca, P.U. Sauer, Phys. Rev. C 72 (2005) 054004.
[45] W. Grüebler, V. König, P.A. Schmelzbach, B. Jenny, J. Vybiral, Nucl. Phys. A 369 (1981) 381.
[46] P. Guss, K. Murphy, R. Byrd, C. Floyd, S. Wender, R. Walter, T. Clegg, W. Wylie, Nucl. Phys. A 395 (1983) 1.
[47] V. König, W. Grüebler, R. Hardekopf, B. Jenny, R. Risler, H. Bürgi, P. Schmelzbach, R. White, Nucl. Phys. A 331 (1979) 1.
[48] R. Hardekopf, P. Lisowski, T. Rhea, R. Walter, T. Clegg, Nucl. Phys. A 191 (1972) 468.
[49] G. Spalek, R. Hardekopf, J. Taylor Jr., T. Stammbach, R. Walter, Nucl. Phys. A 191 (1972) 449.